Two-photon photophysical properties of tri-9-anthrylborane

ARTICLE *in* CHEMICAL PHYSICS LETTERS · FEBRUARY 2007

Impact Factor: 1.9 · DOI: 10.1016/j.cplett.2007.01.034

Available online at www.sciencedirect.com
ScienceDirect
Chemical Physics Letters 436 (2007) 280–286
CHEMICAL PHYSICS LETTERS
www.elsevier.com/locate/cplett

Two-photon photophysical properties of tri-9-anthrylborane

Xue-Fei Wang [a,b], Xin-Ran Zhang [c], Yi-Shi Wu [a,b], Jian-Ping Zhang [a,b,*], Xi-Cheng Ai [b,*], Yuan Wang [c,*], Meng-Tao Sun [d]

[a] *Beijing National Laboratory for Molecular Science (BNLMS), State Key Laboratory for Structural Chemistry of Unstable and Stable Species, Institute of Chemistry, Chinese Academy of Sciences, Beijing 100080, China*
[b] *Department of Chemistry, Renmin University of China, Beijing 100872, China*
[c] *College of Chemistry and Molecular Engineering, Peking University, Beijing 100871, China*
[d] *Institute of Physics, Chinese Academy of Sciences, Beijing 100080, China*

Received 29 November 2006; in final form 8 January 2007
Available online 17 January 2007

Abstract

Boron-containing π-conjugated chromophores with unique electronic structures are potent in electro-optical applications, fluorescent chemsensoring and biolabelling. We have done spectroscopic and computational studies on tri-9-anthrylborane (An_3B) aiming at providing a deeper insight into its photophysical properties. The fluorescent properties are found to depend strongly on solvent polarity, whereas the 2-photon absorption cross-section with a maximum of ~110 GM at 805 nm (in *n*-hexane) shows little solvent dependence. The spectroscopic results combined with the theoretical analyses reveal that the lowest excited state is both 1- and 2-photon allowed, while the second lowest excited state is optically dark and strongly 2-photon allowed. This unique electronic structure gives rise to considerably large 2-photon absorption cross-sections for An_3B over a wide spectral range.

1. Introduction

Boron incorporated into π-conjugated molecules can extend the π-electron delocalization via the p_π–π* conjugation and can introduce intramolecular charge transfer (ICT) owing to its electron-withdrawing nature [1]. Therefore, boron-containing π-conjugated molecules bear unique luminescent, nonlinear optical, electrochemical and electron transporting properties [2], and anticipate a range of applications such as in (eletro)luminescence [3], nonlinear optics [4], optical switching [5], fluorescent biolabelling [6] and photosensitizers of photo-dynamic therapy [7]. It has also been demonstrated that boron-containing chromophores can be used as fluorescent chemosensors, since the p_π–π* conjugation is susceptible to electron donating species such as anions or some organic solvents, which leads to dramatic change of fluorescence wavelength and quantum yield [8–12].

Tri-9-anthrylborane (Scheme 1, hereafter abbreviated as An_3B) was originally synthesized and characterized by Yamaguchi et al. [11]. These authors found that the HOMO of this molecule is primarily localized on specific anthryls, whereas the LUMO is equally delocalized to three anthryls with the highest electron density at the boron center. Therefore, when the electron system is promoted from HOMO to LUMO upon optical excitation, the ICT-type electronic transition from the peripheral anthryls to the central boron takes place. In addition, it is of practical importance that An_3B exhibits good chemical stability both in air and against water because the tri-coordination of boron are saturated [11]. In analogy to An_3B, a number of three-coordinate boron-centered compounds were reported, e. g., triarylborane [12], triphenylboron [13] and tridurylborane [10], and their photophysical and photochemical properties were investigated.

* Corresponding authors. Address: Beijing National Laboratory for Molecular Science (BNLMS), State Key Laboratory for Structural Chemistry of Unstable and Stable Species, Institute of Chemistry, Chinese Academy of Sciences, Beijing 100080, China. Fax: +86 10 62516604 (J.-P. Zhang).
E-mail address: jpzhang@mail.iccas.ac.cn (J.-P. Zhang).

0009-2614/$ - see front matter © 2007 Elsevier B.V. All rights reserved.
doi:10.1016/j.cplett.2007.01.034

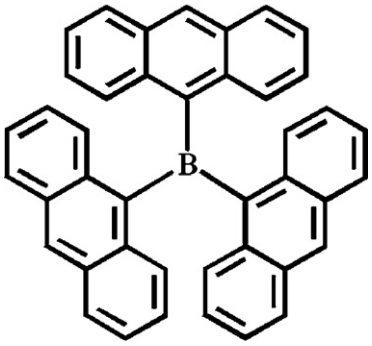

Scheme 1. The molecular structure of tri-9-anthrylborane (An_3B).

Recently, the electronic structure and the 1-photon photophysics of An_3B have been extensively studied [14–16]. Optical excitation into the characteristic lowest-energy and featureless absorption band results in the electronic excitation with ICT character, which endows An_3B considerably large change of static dipole moments (8.0 D) [14,15] as well as large transition dipole moments (~4.8 D, this work), therefore, significant nonlinear optical response of this compound may be expected. In the present work, we have attempted to investigate An_3B's 1- and 2-photon photophysical properties with an emphasis on their correlation, as well as on the 2-photon photophysical behavior. Considerably large 2-photon absorption (2PA) cross-section was observed over a wide spectral range, and an optically forbidden state showing the largest 2PA cross-section was newly revealed for An_3B. Furthermore, the 2-photon fluorescence excitation spectrum was found to be insensitive to the change of solvent polarity. These 2-photon characteristics combined with the remarkable solvatochromism of fluorescence may be useful for the potential use of this compound in 2-photon fluorescent chemosensoring or biolabelling.

2. Materials and methods

2.1. Synthesis of An_3B

An_3B was synthesized following the procedure described in Ref. [11] with certain modifications. Briefly, an ether solution (5 ml) of $BF_3 \cdot OEt_2$ (426 mg, 3 mmol) was added to a suspension of 9-anthryllithium, which was prepared from 9-bromoanthracene (2.57 g, 10 mmol) and *n*-BuLi (1.6 M hexane solution, 6.5 ml, 10.5 mmol) in ether (15 ml) at 0 °C. The reaction mixture was stirred for 12 h at room temperature. The orange precipitates produced were collected by filtration and washed with ether (5 ml × 2), benzene (250 ml) was then added to the precipitates and the resulting suspension was stirred and filtered to remove the insoluble solids. Column chromatography was used to separate the main product from the by-products, for which 1,2-dichloroethane was used as the eluent. The target compound was finally recrystallized from benzene to afford pure product appearing as orange crystals (0.78 g, 1.44 mmol, 48% yield). Anal. Calc. for $C_{42}H_{27}B$: C 92.50 (92.99), H 5.04 (5.02). ^1H NMR ($CDCl_3$, room temperature) δ 8.54 (s, 3H), 8.06 (d, $J = 8.7$ Hz, 6H), 7.97 (d, $J = 8.6$ Hz, 6H), 7.28–7.24 (m, 6H), 6.91–6.88 (m, 6H). EI-MS Calc. for $C_{42}H_{27}N_3O_6$: 542.5, found: 542.3 (M^+).

2.2. Linear spectroscopic measurements

An absorption spectrometer (U-3310, Hitachi) and a fluorescence spectrophotometer (F-2500, Hitachi) were used to record room-temperature UV–Vis absorption and fluorescence spectra, respectively. Time-resolved fluorescence spectroscopy was performed at room temperature by the use of a photon-counting type streak camera (C2909, Hamamatsu Photonics) with a time resolution of 500 ps, and the pulsed excitation light at 470 nm were supplied by an optical parametric amplifier (OPA-800CF, Spectra Physics) pumped by the output (800 nm, ~120 fs, 0.7 mJ, 1 kHz) from a regenerative amplifier (Spitfire, Spectra Physics). Spectroscopic grade solvents were used in the spectroscopic experiments without further purification.

2.3. 2-Photon spectroscopic measurements

Laser pulses in the wavelength range of 700–1000 nm for 2-photon excitation (2PE) were provided by the aforementioned optical parametric amplifier, and the pulse energy was monitored by using an optical power meter (Model 372, Scientech). The 2PE-induced fluorescence was collected with a 90-degree geometry and recorded with a liquid nitrogen cooled CCD detector (SPEC-10-400B/LbN, Roper Scientific) attached to a polychromator (SpectraPro-500i, Acton).

The 2PA cross-section (δ) of An_3B was obtained following the method described in Ref. [17] by the use of the relation,

$$\delta_s = \delta_r \frac{\eta_r I_r^2 C_r \Phi_r F_s n_s^2}{\eta_s I_s^2 C_s \Phi_s F_r n_r^2},$$

where η and I, respectively, represent the collection efficiency of the optical system and the intensity of the incident light ($\eta_s = \eta_r$; $I_s = I_r$). C stands for the sample concentration, Φ for the fluorescence quantum yield, F for the integrated intensity of the 2PE induced fluorescence and n for the refractive index of solvent. Subscripts s and r refer to sample and reference, respectively. 2-Photon fluorescent fluorescein in water (pH 13) with known 2PA cross-section ($\delta_{800\ nm} = 33$ GM) [18] was used as the reference.

2.4. Quantum chemical calculations

Quantum chemical calculations for An_3B were carried out by the use of the GAUSSIAN03 suite [19]. Geometry optimization for the ground state An_3B was performed with HF/6-31G. The optimization result showed that three anthryl subchromophores arrange in a trigonal and

propeller-like manner with a dihedral angel of 52.3°, in well agreement with the crystallographic data (53°) [11]. The transition energy and oscillator strength were calculated with the time-dependent DFT [20], the B3LYP functional and the 6-31+G basis set. The nice agreement between the theoretical results and the spectral observations indicates that the calculations are reliable. The excited-state properties of An_3B were characterized and investigated with the three-dimensional cube representation of the charge difference density (CDD) [21,22], which shows the distribution of net change in electron density as a result of electronic transition and the orientation of the possible ICT process.

3. Results and discussion

3.1. 1-Photon photophysical properties

The linear absorption spectrum of An_3B in Fig. 1 exhibits three major features peaked at 470 nm (band-I), 360 nm (band-II) and 290 nm (band-III), in complete agreement with those reported in Refs. [11,14,15]. We have calculated the transition energies and oscillator strengths by the use of time-dependent DFT/B3LYP/6-31+G, and the results are listed in Table 1. Transition energies thus obtained appear to be red shifted for ~22 nm with respect to experimental values, which is understandable in view of the fact that the solvent effect and vibrational state were not taken into account in the calculations [23]. Here, we note that time-dependent DFT/B3LYP combined with 3-21G and 6-31G also yielded reasonable results, indicating rather weak dependence on the choice of basis sets. However, theoretical predictions obtained by the use of the time-dependent HF deviated substantially from the spectral observations.

Optical transitions that constitute the absorption band-I are those to the S_1 and the S_2 state carrying large oscillator strengths (Table 1). The characteristics of the electronic transitions to the S_1 and the S_2 states are illustrated by the CDD patterns in Fig. 2, which clearly show the anthryl-to-boron ICT characters. It is seen from Table 1 that S_1 and S_2, to which the electronic transitions are strongly 1-photon allowed, are practically degenerate in transition energy. However, the transition to S_3 is essentially 1-photon forbidden owing to the vanishingly small oscillator strength. These results can be well understood within the framework of exciton coupling theory that applied successfully to the D_3-symmetric ground-state An_3B [15] and to the structural analogues of An_3B such as triarylborane [12] and triphenylamine [24]. In the weak-coupling regime, the low-lying excited states split into a set of degenerate E state (S_1 and S_2) and an A state (S_3) owing to the transition dipole–transition dipole interaction between the anthryl subchromophores.

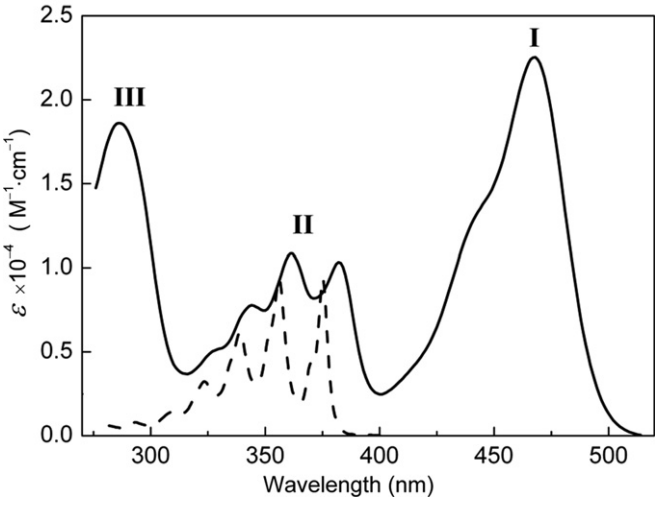

Fig. 1. The 1-photon absorption spectrum of An_3B in *n*-hexane (solid curve), and that of anthracene in the same solvent (dashed curve) for comparison.

Table 1
Calculated transition wavelengths (λ_{cal}, nm) and oscillator strengths (f) of 12 singlet-excited states of An_3B

State	λ_{cal}	f	λ_{obs}
S_1	**492.92**	**0.1006**	470
S_2	**492.89**	**0.1006**	
S_3	434.08	0.0000	
S_4	395.41	0.0004	365
S_5	**388.08**	**0.0613**	
S_6	**388.07**	**0.0614**	
S_7	365.83	0.0000	290
S_8	**353.92**	**0.0288**	
S_9	**353.93**	**0.0288**	
S_{10}	**343.99**	**0.0105**	
S_{11}	**343.97**	**0.0105**	
S_{12}	**333.96**	**0.0079**	

The observed absorption wavelengths (λ_{obs}, nm) are taken from the linear spectrum of An_3B in Fig. 1. Transitions of large oscillator strengths are shown in bold.

The ICT characters of electronic excitations associated with band-I are corroborated by a solvent-effect test, the results of which are listed in Table 2. The absorption maximal wavelength (λ_A) of band-I exhibits a bathochromic shift for less than 10 nm with reference to *n*-hexane solution, whereas the bathochromic shift of the fluorescence wavelength (λ_F) and the Stokes shift ($\Delta\lambda$) increase systematically upon increasing the solvent polarity. In addition, the fluorescence quantum yield (Φ) and lifetime (τ) decrease monotonically when the solvent polarity gets higher. These photophysical behavior reflect the ICT characters of the emissive excited states [14,15]. The lack of solvatochromism in the 1-photon absorption was also observed for three-coordinate tridurylboranes, which was attributed to the highly polarized excited state produced by the ICT transition [10]. Most recently, Lambert and co-workers reported pronounced negative solvatochromism in the ICT absorptive band of the amino substituted triarylboranes, and ascribed the phenomenon to dipole inversion upon optical excitation, as well as to the breaking down of D_3 symmetry in the ground and the excited state [12].

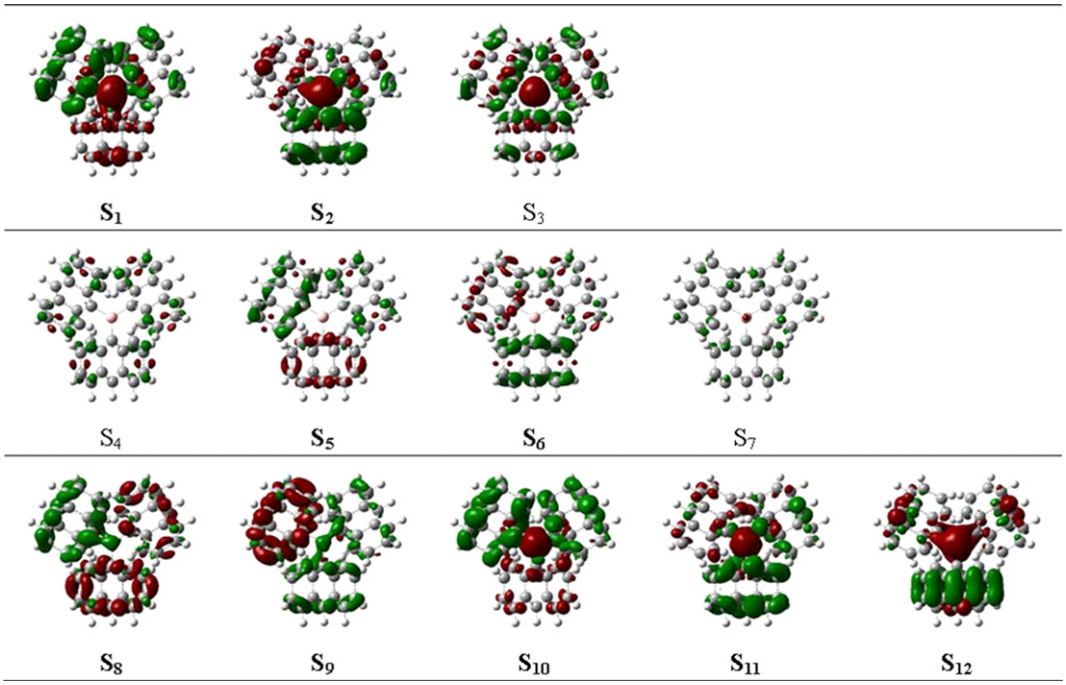

Fig. 2. The isodensity plots of CDDs for transitions to 12 singlet-excited states. The negative density (green) corresponds to hole and the positive (red) to electron. The CDDs are categorized in to three groups (rows) according to the similarities in the electron/hole density at the central boron and in the transition energies.

Table 2
1-Photon photophysical parameters of An_3B

Solvent	P[a]	λ_A	λ_F	$\Delta\lambda$[b]	$\varepsilon/10^4$	Φ[c]	τ
n-hexane	0.229	468	507	39	2.24	0.300	9.3 ± 0.8
Benzene	0.295	476	522	46	2.17	0.140	6.2 ± 0.7
1,2,4-trichlorobenzene	0.521	477	520	43	1.94	0.086	
Tetrahydrofuran	0.687	472	530	58	2.19	0.047	3.8 ± 0.5
Acetone	0.868	470	540	70	2.02	0.014	1.5 ± 0.1
Ethanol	0.886	469	532	63	1.96	0.014	1.2 ± 0.1
Methanol	0.913	468	531	63	2.00	0.011	0.9 ± 0.1
Acetonitrile	0.921	472	543	71	2.07	0.007	1.1 ± 0.1

Wavelengths of absorption and fluorescence maxima (λ_A and λ_F, nm), maximal extinction coefficient (ε, mol^{-1} cm^{-1}), fluorescence quantum yield (Φ) and decay lifetime (τ, ns).

[a] Solvent polarity $P = (\varepsilon - 1)/(\varepsilon + 2)$, where ε stands for dielectric constant.

[b] Stokes shift $\Delta\lambda \equiv \lambda_F - \lambda_A$.

[c] Fluorescence quantum yield referring to fluorescein with $\Phi = 0.9$ in water (pH 13) [18].

The absorption band-II (360 nm, Fig. 1) with clear vibronic progression closely resembles the characteristic absorption of isolated anthracene, and can be attributed to the π-electron system of the anthryl moieties. The 6-nm red shift and the slight broadening of the vibronic bands of An_3B with respect to free anthracene are most likely due to the electronic interaction and the structural heterogeneity among the subchromophores. This band originates from the absorptive transitions to S_5 and S_6 judging from the transition energies and the sizable oscillator strengths (Table 1). The CDDs of S_5 and S_6 in Fig. 2 clearly indicate the anthryl-to-anthryl ICT characters and, in contrary to the S_1 and S_2 states, the central boron is not involved in these anthryl-localized excitations. The absorption band-III (290 nm, Fig. 1), not existing for free anthracene, can be ascribed to the electronic excited states S_8 through S_{12}, among which S_8 and S_9 carry significant oscillator strengths (Table 1). All of these five states bear pronounced ICT characters involving the central boron.

Here we note that the above 1-photophysical properties of An_3B are in general agreement with those recently reported by Kitamura et al. on the basis of detailed spectroscopic studies [14,15] These authors ascribed the absorptive bands I and II, respectively, to the ICT-type excited state and to the anthryl-localized excited state, while band III to the ICT-type higher-lying excited state. The present experimental and theoretical results corroborate to Kitamura and coauthors', and emphasize on the pronounced ICT

characteristics of electronic excitations introduced by the central boron, which is to be related to the 2-photon photophysical properties of An_3B.

3.2. 2-Photon photophysical properties

Fig. 3 compares the 1- and 2-photon fluorescence excitation spectra as well as the 1- and 2-photon induced fluorescence spectra of An_3B. The 1-photon induced fluorescence spectrum exhibits an intense band at 507 nm, and appears as a mirror-image of the 1-photon fluorescence excitation spectrum. Bands I and II of the 1-photon fluorescence excitation spectrum in Fig. 3 agree well with those of the linear absorption spectrum in Fig. 1 in terms of relative intensity and overall spectral pattern, a fact which proves efficient internal conversion from the anthryl localized S_5 and S_6 to the lowest S_1 and S_2 states. However, a close comparison between the 1-photon fluorescence excitation and the linear absorption spectra reveals that band-I of the former has more and clearer fine structures than the latter, which implies that more than one excited states are responsible for this band [17]. This is indeed supported by the theoretical results as discussed above. For band-I, the 1- and 2-photon fluorescence excitation spectra are rather similar in spectral shape, indicating that optical transitions constituting this band are both 1- and 2-photon allowed, a case which is rather common for dye molecules undergoing significant change of static dipole moments and having large transition dipole moments associated to the ICT-type optical excitations [25,26].

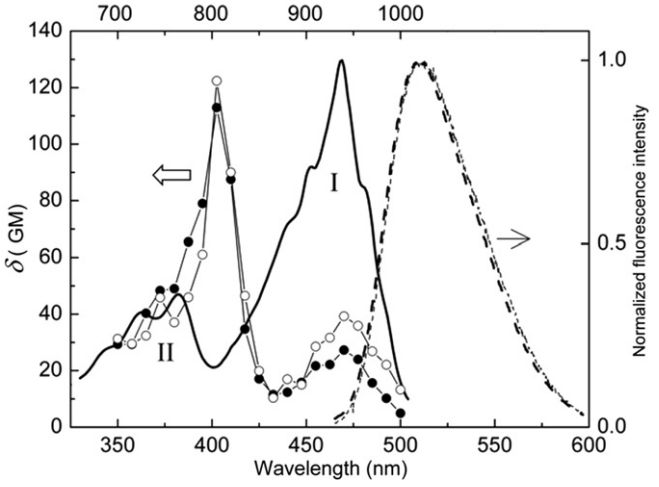

Fig. 3. The 1-photon fluorescence excitation spectrum (solid curve, main spectral bands are labeled with I and II), and the 2-photon fluorescence excitation spectra of An_3B in *n*-hexane (filled circle) and in tetrahydrofran (open circle). Magnitudes of the 1PE-induced (dotted curve, $\lambda_{exc} = 450$ nm), the 2PE-induced (dashed curve, $\lambda_{exc} = 800$ nm) fluorescence spectra and the 1-photon fluorescence excitation spectrum are arbitrarily scaled. Upper abscissa for the 2-photon fluorescence excitation spectra is simply the doubling of linear absorption wavelength. The quadratic dependence (slope, 2.0 ± 0.1) of the 2PE-induced fluorescence intensity on the excitation laser power was confirmed. 1 GM = 10^{-50} cm^4 s photon^{-1} molecule^{-1} [18].

The 2PA cross-section of An_3B has a maximum of ~110 GM at ~805 nm as seen from the 2-photon fluorescence excitation spectrum in Fig. 3. This intensive 2PA feature is most probably originated from the 2-photon-allowed S_3 state with obvious ICT character (Fig. 2). Interestingly, the strongest 2PA feature does not present at the transition wavelengths of band-I where 1PA is the strongest, although the optical transitions of band-I are both 1- and 2-photon allowed. The 1-photon transition to the S_3 state carries vanishingly small oscillator strengths (Table 1), however, this state can be readily detected by 2-photon fluorescence excitation spectroscopy that is complementary to 1-photon spectroscopy [27]. Our 2-photon spectroscopic results thus disclose the optically hidden state of An_3B (S_3).

An_3B is an octupolar molecule consisting of an electron-withdrawing boron center and three electron-releasing peripheral anthryls. The periphery-to-center ICT character of the S_1 and S_2 states combined with the large transition dipole moments (4.77 D, 3.96 D and 3.90 D for bands I, II and III, respectively) give rise to considerably large 2PA cross-section over a wide wavelength range [26,28], and may also facilitate other types of nonlinear optical response [24,29]. The action cross-section as defined by the product of 2PA cross-section (δ) and the fluorescence quantum yield (Φ) is $\delta \cdot \Phi \sim 33$ GM. This value is comparable to those of fluorescein [18] and europium complexes such as the recently reported one with tris(6,6,7,7,8,8,8-heptafluoro-2,2-dimethyl-3,5-octanedionato) and Michler's ketone as ligands [30], and is much higher than most of the endogenous biological chromophores [31].

As seen in Fig. 3, the 2-photon fluorescence excitation spectrum of An_3B in moderately polar tetrahydrofran resembles closely to that in nonpolar *n*-hexane, showing little change in the 2PA cross-sections. To the contrary, the effective 2PA cross-section of the asymmetric polar molecule AF50 decreases upon increasing the solvent polarity, which has been ascribed to the influence of molecular environment on the solvent-stabilization of the longest-lived 1-photon-excited state [32]. Recent investigations have demonstrated prominent solvent effects on the 2PA property of chromophores, for which the detailed mechanisms are awaiting further theoretical and experimental studies [33,34]. For instances, for distyrylbenzene derivatives dissolving in organic solvents and water, Woo et al. observed an increase in the 2PA cross-section followed by a systematic decrease upon increasing the solvent polarity, and a maximal 2PA action cross-section was found in solvents of moderate polarities [34]. These authors explained the observation in terms of the solvent effect on the ICT magnitude as proposed by Wang et al. [35], and suggested the existence of specific solute–solvent interaction, such as hydrogen bonding, to account for some substantial deviations. In a quantum chemical investigation on model push-pull 2PA chromophores, Bartkowiak et al. proved the change in the bond length alteration of the conjugation owing to the polarization effect from polar surroundings, and found that the 2PA cross-section, as well as the first-

and second-order hyperpolarizabilities are all solvent dependent [33].

In discussing the lack of solvent dependence of 2PA cross-section found for An_3B in the present study, we consider the two major 2PA-bands at 805 nm and 940 nm, respectively. (i) On going from *n*-hexane to tetrahydrofran, the 805-nm band shows little difference within experimental error. The S_3 state associated with this band is optically-forbidden but accessible via the S_0-to-S_3 2PA transition (*vice supra*). It is known that the ground-state An_3B possess negligible static dipole moment for symmetric reasons [15]. On the other hand, the totally-symmetric CDD pattern of S_3 implies a negligible change in static dipole moment upon the 2PA transition (Fig. 2), and hence the static dipole moment of the S_3 state is also negligible. Therefore, the effective electric field from surroundings can hardly polarize the ground- or the S_3-state An_3B, i.e. the ICT character associated with the S_0-to-S_3 2PA transition is not sensitive to the change of solvent polarity. (ii) For the 940-nm band originated from the degenerated and 1- and 2-photon-allowed S_1 and S_2 states, the corresponding CCDs are of lower symmetry with reference to S_3 (Fig. 2). In this case, the ICT can be perturbed by the electric polarization exerted by polar solvents. According to Bartkowiak and coauthors' theoretical work, polar environment may facilitate the ICT when the polarization of the chromophore parallels the orientation of ICT [33]. For the 940-nm band, our data indeed show a slight increase of 2PA cross-section on going from *n*-hexane to tetrahydrofran (Fig. 3), which analogues Woo's recent observation that a neutral distyrylbenzene derivative (**8N**) exhibited substantially higher 2PA cross-section in tetrahydrofran than that in toluene [34].

The observation of solvent-independence of the 2PA band of An_3B at 805 nm provides an exception of the general trend of solvent-dependence of 2PA established for many other chromophores [34], the underlying mechanism, however, is not fully understood. An_3B is unique in its insensitivity of 2PA in response to the change of solvent environments, and in its large 2PA action cross-section over a wide range of spectral region, this combined with the large solvatochromism in fluorescence may be advantageous for An_3B to be used in 2-photon fluorescent chemosensoring and biolabelling.

To summarize, we have investigated and characterized the electronic excited states responsible for the 1- and 2-photon photophysical properties of An_3B both experimentally and theoretically. Spectroscopic results show that its fluorescent behavior, i.e. the transition wavelength, quantum yield and lifetime, are very sensitive to solvent polarity, whereas its 2PA cross-section with a maximal value of ~110 GM at 805 nm shows little solvatochromism. In addition, an optically forbidden state responsible for the largest 2PA cross-section of this compound was newly identified. Quantum chemical analyses reveal that the central boron atom results in rich manifolds of electronic excited states with ICT characters. The unique electronic structure of An_3B leads to considerably large 2PA cross-sections over a wide spectral range. The 2-photon photophysical properties of An_3B combined with its remarkable fluorescence solvatochromism may be useful for widening the potential applications of this compound.

Acknowledgements

We are grateful for the Grants-in-Aid from the NSFC (Grants 20433010, 90606017, 50521201, 20673144), NKBRSF (2006CB806102), and the RFDP from the Ministry of Education of China. Financial support from the Knowledge Innovation Program of the Chinese Academy of Sciences is also acknowledged. M.T. Sun is indebted to the financial support from Wenner-Gren Foundation of Sweden.

References

[1] N. Matsumi, K. Naka, Y. Chujo, J. Am. Chem. Soc. 120 (1998) 5112.
[2] T. Noda, Y. Shirota, J. Am. Chem. Soc. 120 (1998) 9714.
[3] X.T. Tao, H. Suzuki, T. Wada, S. Miyata, H. Sasabe, J. Am. Chem. Soc. 121 (1999) 9447.
[4] C. Branger, M. Lequan, R.M. Lequan, M. Large, F. Kajzar, Chem. Phys. Lett. 272 (1997) 265.
[5] Z.Q. Liu, M. Shi, F.Y. Li, O. Fang, Z.H. Chen, T. Yi, C.H. Huang, Org. Lett. 7 (1996) 5481.
[6] N. Malatesti, R. Hudson, K. Smith, H. Savoie, K. Rix, K. Welham, R.W. Boyle, Photochem. Photobiol. 82 (2006) 746.
[7] J.S. Hill, S.B. Kahl, S.S. Stylli, Y. Najanyra, M.S. Koo, A.H. Kaye, Proc. Natl. Acad. Sci. USA 92 (1995) 12126.
[8] S. Yamaguchi, S. Akiyama, K. Tamao, J. Am. Chem. Soc. 123 (2001) 11372.
[9] S. Yamaguchi, T. Shirasaka, S. Akiyama, K. Tamao, J. Am. Chem. Soc. 124 (2002) 8816.
[10] S. Yamaguchi, T. Shirasaka, K. Tamao, Org. Lett. 2 (2000) 4129.
[11] S. Yamaguchi, S. Akiyama, K. Tamao, J. Am. Chem. Soc. 122 (2000) 6335.
[12] Stahl, R. Lambert, C. Kaiser, C. Wortmann, R. Jakober, R. Chem. Eur. J. 12 (2006) 2358.
[13] H. Slama, C. Brauchle, J. Voitlander, Chem. Phys. Lett. 102 (1982) 307.
[14] N. Kitamura, E. Sakuda, J. Phys. Chem. A 109 (2005) 7429.
[15] N. Kitamura, E. Sakuda, T. Yoshizawa, T. Iimori, N. Ohta, J. Phys. Chem. A 109 (2005) 7435.
[16] E. Sakuda, K. Tsuge, Y. Sasaki, N. Kitamura, J. Phys. Chem. A 109 (2005) 22326.
[17] B.R. Cho et al., J. Am. Chem. Soc. 123 (2001) 10039.
[18] M.A. Albota, C. Xu, W.W. Webb, Appl. Optics. 37 (1998) 7352.
[19] M.J. Frisch et al., Gaussian03, Revision B.05, Gaussian Inc., Pittsburgh, PA, 2003.
[20] E.K.U. Gross, W. Kohn, Phys. Rev. Lett. 55 (1985) 2850.
[21] N.K. Persson, M.T. Sun, P. Kjellberg, T. Pullerits, O. Inganäs, J. Chem. Phys. 123 (2005) 204718, 1–9.
[22] M.T. Sun, J. Chem. Phys. 124 (2006) 054903, 1–6.
[23] M. Belletete, J.F. Morin, M. Leclerc, J. Phys. Chem. A 109 (2005) 6953.
[24] C. Lambert, W. Gaschler, E. Schmalzlin, K. Meerholz, C. Brauchle, J. Chem. Soc. Perkin. Trans. 2 (1999) 577.
[25] P. Porres, O. Mongin, C. Katau, M. Charlot, T. Pons, J. Mertz, M.B. Desce, Org. Lett. 6 (2004) 47.
[26] B. Dick, G.J. Hohlneicher, Chem. Phys. 76 (1982) 5755.
[27] L. Goodman, R.P. Rava, Acc. Chem. Res. 17 (1984) 250.
[28] J. Zimmermann, P.A. Linden, H.M. Vaswani, R.G. Hiller, G.R. Fleming, J. Phys. Chem. B 106 (2002) 9418.

[29] S. Kim, K.H. Song, S.O. Kang, J. Ko, Chem. Commun. (2004) 68.
[30] M.H.V. Werts, N. Nerambourg, D. Pélégry, Y.L. Grand, M.B. Desce, Photochem. Photobiol. Sci. 4 (2005) 531.
[31] W.R. Zipfel, R.M. Williams, W.W. Webb, Nature Biotechnol. 21 (2003) 1369.
[32] J.W. Baur et al., Chem. Mater. 11 (1999) 2899.
[33] W. Barthowiak, R. Zalesny, J. Leszczynski, Chem. Phys. 287 (2003) 103.
[34] H.Y. Woo, B. Liu, B. Kohler, D. Korystov, A. Mikhailovsky, G.C. Bazan, J. Am. Chem. Soc. 127 (2005) 14721.
[35] C.K. Wang, K. Zhao, Y. Su, Y. Ren, X. Zhao, Y. Luo, J. Chem. Phys. 119 (2003) 1208.